GaN-based photonic crystal surface emitting lasers with central defects

Tzeng-Tsong Wu, Peng-Hsiang Weng, Yen-Ju Hou, and Tien-Chang Lu

Articles you may be interested in

GaN-based surface-emitting laser with two-dimensional photonic crystal acting as distributed-feedback grating and optical cladding
Appl. Phys. Lett. **97**, 251112 (2010); 10.1063/1.3528352

Lasing characteristics at different band edges in GaN photonic crystal surface emitting lasers
Appl. Phys. Lett. **96**, 071108 (2010); 10.1063/1.3313947

Characteristics of GaN-based photonic crystal surface emitting lasers
Appl. Phys. Lett. **93**, 111111 (2008); 10.1063/1.2986527

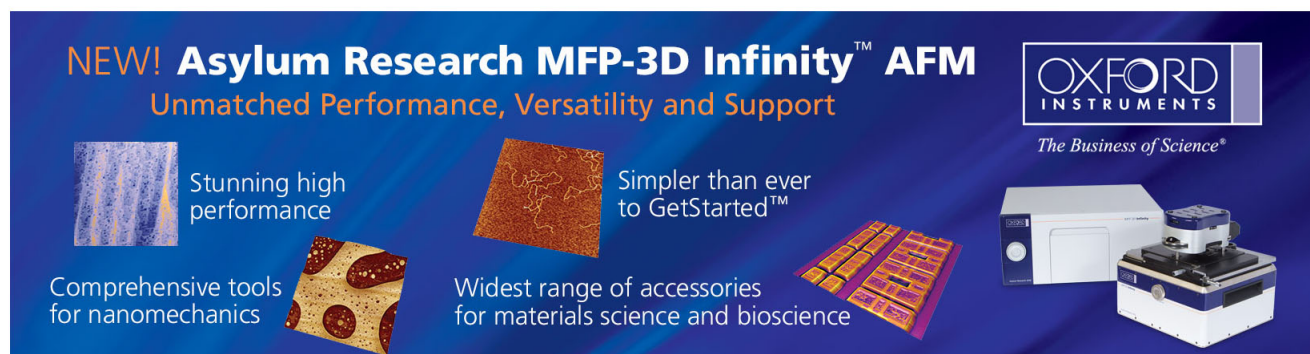GaN-based two-dimensional surface-emitting photonic crystal lasers with Al N Ga N distributed Bragg reflector
Appl. Phys. Lett. **92**, 011129 (2008); 10.1063/1.2831716

Coherent coupling of two-dimensional arrays of defect cavities in photonic crystal vertical cavity surface-emitting lasers
Appl. Phys. Lett. **86**, 201104 (2005); 10.1063/1.1929074

GaN-based photonic crystal surface emitting lasers with central defects

Tzeng-Tsong Wu, Peng-Hsiang Weng, Yen-Ju Hou, and Tien-Chang Lu[a)]

Department of Photonics and Institute of Electro-Optical Engineering, National Chiao Tung University, Hsinchu 30050, Taiwan

The GaN-based photonic crystal surface emitting lasers (PCSELs) with different central defects were fabricated and investigated. The threshold energy densities increased from 3.23 to 3.51 mJ/cm^2 when the central defect size increased. In addition, lasing wavelengths decreased from 400 nm to 390 nm due to the guided mode shifting phenomenon for the PCSEL cavities with larger central defects. The tendency of threshold gain and resonance wavelength for PCSELs with different central defects were calculated by the multiple scattering method and well matched to the experimental results. © 2011 American Institute of Physics. [doi:10.1063/1.3665251]

Photonic crystal lasers based on the band edge effect have attracted much attention because of their superior advantages such as high power emission, single mode operation, and coherence oscillation over a large area.[1–3] The photonic crystal lasers with designed lattice constant and radius could produce surface emitting condition at the band edges by satisfying the specific Bragg condition.[4,5] These kinds of photonic crystal surface emitting lasers (PCSELs) usually compose of a well-defined pattern and photonic crystal lattice over a large area. So far, many kinds of PCSELs with emission wavelength ranged from UV to IR bands have been developed during the past decade.[6–10] On the other hand, membrane type photonic crystal lasers with defect cavities are usually formed by removing central air holes surrounded by a less PC area. Due to the band gap effect in the lateral direction and total internal reflection in the vertical direction, it could achieve a small mode volume with a high quality factor and strong-coupling effect. This kind of defect laser has also been realized in several kinds of materials such as InGaAsP and InP material systems due to their availability to form membrane structures.[11,12] However, few studies reported the effect of the central defect on the band edge mode PCSELs. In this letter, the GaN-based PCSELs with different central defects have been fabricated and measured to understand the effect of central defects on lasing characteristics of PCSELs. The band edge mode at Γ point could be disturbed by varying the central defect sizes. Different threshold energy density and lasing wavelength for different central defects were obtained. The dispersion diagrams of PCSELs with different central defects are also investigated. Finally, we employed the multiple scattering methods to calculate the threshold gain and resonance wavelength of the PCSLEs with different central defects. The simulation results show similar tendency to the experimental results.

The GaN-based PCSELs were grown by a metal-organic chemical vapor deposition system (EMCORE D-75) on a c-plane 2-in sapphire substrate. The epitaxial structure consists of a 25 pairs AlN/GaN distributed Bragg reflectors (DBRs), a 560 nm-thick n-GaN layer, 10 pairs of InGaN/GaN multiple quantum wells (MQWs), a 24 nm-thick AlGaN electron blocking layer, and a 175 nm-thick p-GaN layer. The detailed growth parameters are reported elsewhere.[13] The typical photoluminescence (PL) spectrum of MQWs had a peak centered at a wavelength of 415 nm with a linewidth of about 25 nm. Then, the photonic crystals with triangular lattice were patterned by e-beam lithography. The photonic crystal patterns were etched down to a depth of 400 nm through the MQWs layer by using inductively coupled plasma dry etching. The total area of photonic crystal region is about 50 μm. The filling factor and radius of photonic crystal are 0.21 and 40 ~ 50 nm. Fig. 1(a) shows the schematics of GaN-based PCSELs with central defects varied from H0 to H5 in the center of the photonic crystal region. The number after H represents the circle numbers removed from the central photonic crystal lattice, as shown in Fig. 1(b).

The 325 nm continuous wave (CW) He–Cd laser and the 355 nm pulse Nd:YVO$_4$ laser with a pulse width of ∼0.5 ns at a repetition rate of 1 kHz were used as the optical pumping sources in the angular resolved photoluminescence (ARPL) system. All the experiments were carried out at room temperature. The laser beam pumped obliquely onto the GaN-based PCSELs devices with a spot size of about 50 μm to cover the whole photonic crystal pattern. The PL signal was collected by a 15X objective lens normal to the sample surface or by a fiber with a 600 μm core rotating in the normal plane of the sample along the Γ-K direction of triangular lattice and fed into a spectrometer with a charge-coupled device (Jobin-Yvon IHR320 Spectrometer). The spectral resolution was about 0.07 nm for spectral output measurement. The angle resolution was about 0.5°.

The input-output characteristics and the lasing spectra of H0, H3, H4, and H5 defect structures are shown in Fig. 2. Fig. 2(a) shows the input-output characteristic curves of
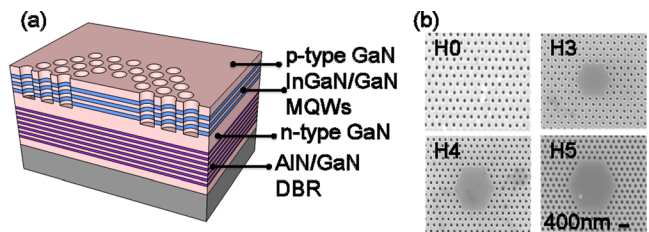

FIG. 1. (Color online) (a) The schematic device structure of GaN-based PCSELs. (b) The plan-view SEM images of no-defect (H0), H3, H4 and H5 central defect structures of GaN-based PCSELs.

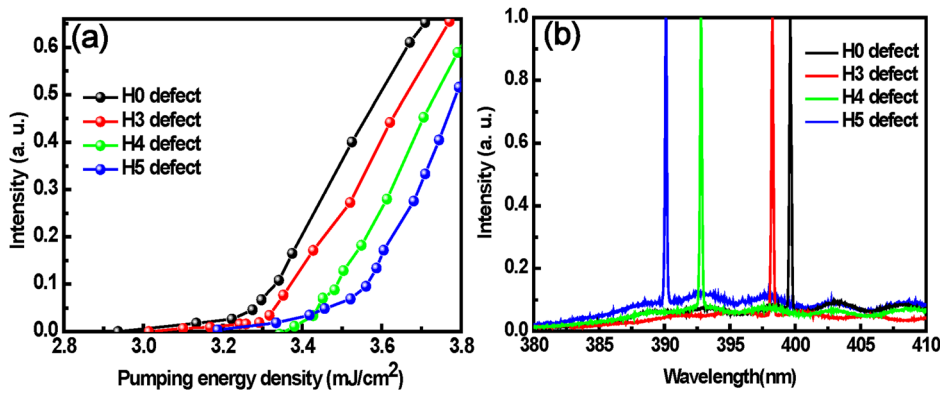[a)]Electronic mail: timtclu@mail.nctu.edu.tw.

FIG. 2. (Color online) (a) Measured output intensity versus input excitation energy density from the GaN-based PCSELs for H0 to H5 defect cavities. (b) Lasing spectrum of different central defect structures including H0, H3, H4, and H5.

PCSELs with different defect cavities of H0, H3, H4, and H5 pumped by the 355 nm pulse Nd:YVO$_4$ laser. The results show that the threshold energy densities are 3.23, 3.3, 3.44, and 3.51 mJ/cm^2 for H0, H3, H4, and H5 defect structures, respectively. These results indicate that the threshold energy density is varied with the central defect area, and the PCSELs with a larger defect size exhibit higher threshold power density. Besides, the quality factors of H0, H3, H4, and H5 defect structures are measured to be 226, 202, 168.5, and 144, respectively. Characteristics of PCSELs with H1 and H2 defects are not shown here, because they are similar to that of the H0 defect. Fig. 2(b) shows the lasing wavelengths of H0, H3, H4, and H5 defect cavity. When the pumping energy density is above threshold of each device, the lasing wavelengths are observed at 400, 398, 392, and 390 nm for H0, H3, H4, and H5 defect cavities. The results show that the lasing wavelength would blue shift when the defect size becomes larger. It also indicates that the lasing wavelength could be tuned by varied with the central defect area.

In order to comprehend more characteristics of GaN-based PCSELs with different central defects, the dispersion curves were measured by the ARPL system (pumped by the 325 nm CW laser) and are shown in Figs. 3(a) to 3(c). The horizontal axis is k//along the Γ-K direction of triangular lattice and the vertical axis is the frequency. Two kinds of dispersion curves are observed in the ARPL diagrams. Fabry–Pérot modes with broad up-ward curves are resulted from the vertical cavity of p-i-n GaN layers and interference of DBR layers. The red solid lines indicate several different ordered guided modes diffracted by the photonic crystal lattice. These diffraction lines can well match to the simulated dispersion curves calculated by the plane wave expansion method using proper effective indices. The Γ band edge positions can be clearly identified in Figs. 3(a) to 3(c) at the cross points of solid lines. These diffraction lines shown in Figs. 3(a) to 3(c) have the same slopes, because these PCSELs have the same fabrication conditions and photonic crystal r/a ratio. However, the positions of the guided modes shift slightly down to smaller frequency when the defect size increases due to the increase in the effective index of PCSELs near the central region.

Figs. 3(d) to 3(f) show the APRL results pumped by the pulse laser above the threshold. The red spot shows the
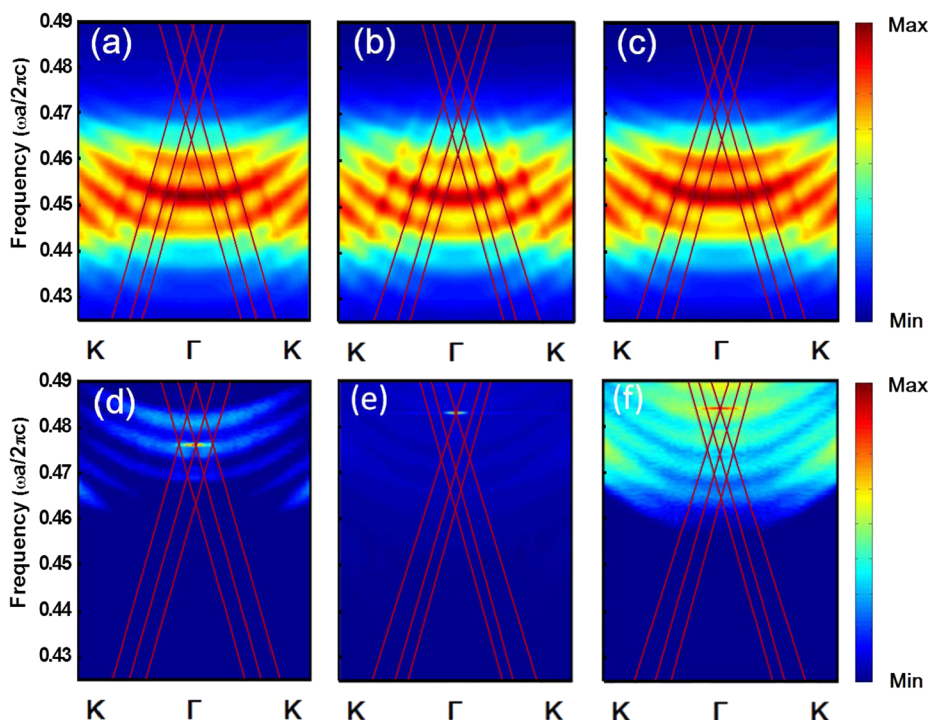

FIG. 3. (Color online) The ARPL diagrams of GaN-based PCSELs for (a) H3, (b) H4 (c) H5 central defects were measured by a 325 nm CW He-Cd laser. The red solid lines represent the calculated diffraction lines for the guide modes. The ARPL diagrams of PCSELs for (d) H3, (e) H4, (f) H5 central defects were measured by a 355 nm Nd:YVO$_4$ pulse laser. The red spots in (d) to (f) represent the lasing frequency at Γ band edge.
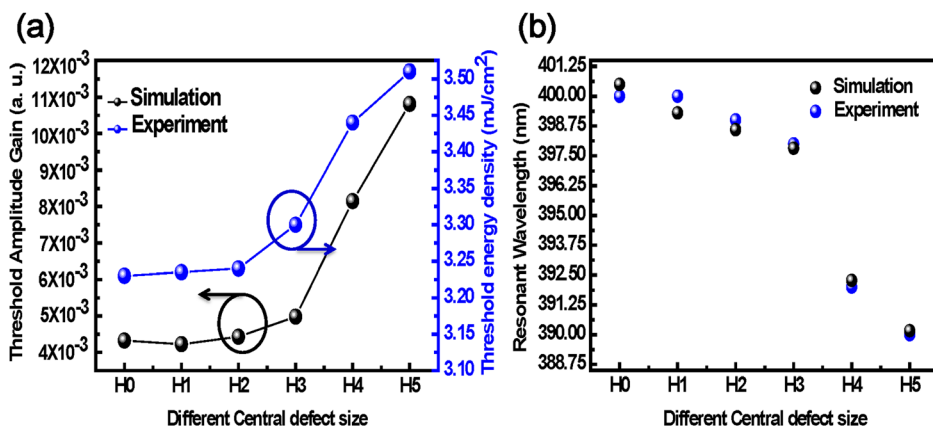
FIG. 4. (Color online) (a) The threshold gain and (b) the resonance wavelength varied with the different defect type from H0 to H5. The black dots and blue dots represent the calculated and experimental results.

lasing frequency. Compared to the PL spectra shown in Figs. 3(a) to 3(c), it should be noted that the PL emission peaks blue shift to a higher frequency due to the screening effect of polarization fields in the InGaN/GaN MQWs when the pumping intensity is high. On the other hand, the diffracted lines remain un-altered. It can be shown that the lasing positions for three different defect cases locate at Γ band edges but with different guided modes. The lasing frequency (0.477) of the PCSEL with H3 defect in Fig. 3(d) belongs to the lower order guided mode. In comparison, the lasing frequency (0.485) of PCSELs with H4 and H5 defects in Figs. 3(e) and 3(f) belongs to the higher order guided mode. This phenomenon of guided mode shifting could be due to the variation of the central defect size. This can be understood by the gain-mode alignment. When the central defect region becomes larger, the band edge position starts to shift downward to smaller frequency due to the increase of the effective index. The gain peak of the MQWs then matches better with the next higher order guided mode. So the lasing peak hops to higher frequency for the PCSELs with H4 and H5 central defects.

The multiple scattering method was carried out to calculate the threshold gains and resonance wavelengths of each device and to compare with the experimental results. The detailed method and simulation parameters were similar to the previous report, and the effective indices of the guided modes were extracted from the experimental data shown in Fig. 3.[14] The lowest threshold gains of PCSELs with different central defects from H0 to H5 are calculated and shown as the black circles in Fig. 4(a). The blue circles indicate the threshold energy densities from the measured results. The resonant wavelengths are also calculated for different defect sizes and compared with experimental results as shown in Fig. 4(b). The relatively large ratios between calculated threshold gains in comparison to those between experimental results are due to limited photonic crystal shell numbers used in our simulation model, and the threshold gain would decay exponentially with the photonic crystal shell numbers. Nevertheless, both simulation and experimental results exhibit similar tendency that the PCSEL with a larger defect size would have a higher threshold due to the less distributed feedback provided by the photonic crystal lattice.

In summary, the GaN-based PCSELs with different central defects have been fabricated and investigated by optical pumping at room temperature. The threshold energy density shows an increasing tendency from 3.23 to 3.51 mJ/cm^2 as the central defect size increases. In addition, the lasing wavelength of each defect cavity shows a blue shift from 400 nm to 390 nm due to the guided mode shifting in PCSELs with different central defects. This has been confirmed by the photonic crystal diffraction lines observed in the ARPL diagrams. Finally, the threshold gains and resonance wavelengths of GaN-based PCSELs with different central defects are calculated by the multiple scattering method. Both the simulation and experimental results show similar tendency that the PCSEL with a larger defect size would have a higher threshold, which could be due to the less distributed feedback provided by the less photonic crystal lattice. These observations can provide a better understanding of the bandedge photonic crystal lasers with central defects.

[1] E. Yablonovitch, Phys. Rev. Lett. **58**, 2059 (1987).
[2] S. John, Phys. Rev. Lett. **58**, 2486 (1987).
[3] M. Meier, A. Mekis, A. Dodabalapur, A. Timko, R. E. Slusher, J. D. Joannopoulos, and O. Nalamasu, Appl. Phys. Lett. **74**, 7 (1999).
[4] M. Imada, A. Chutinan, S. Noda, and M. Mochizuki, Phys. Rev. B **65**, 195306 (2002).
[5] I. Vurgaftman and J. Meyer, IEEE J. Quantum Electron. **39**, 689 (2003).
[6] H. Matsubara, S. Yoshimoto, H. Saito, Y. Jianglin, Y. Tanaka, and S. Noda, Science **319**, 445 (2008).
[7] T. C. Lu, S. W. Chen, L. F. Lin, T. T. Kao, C. C. Kao, P. Yu, H. C. Kuo, S. C. Wang, and S. H. Fan, Appl. Phys. Lett. **92**, 011129 (2008).
[8] S. Kawashima, T. Kawashima, Y. Nagatomo, Y. Hori, H. Iwase, T. Uchida, K. Hoshino, A. Numata, and M. Uchida, Appl. Phys. Lett. **97**, 251112 (2010).
[9] M. Kim, C. S. Kim, W. W. Bewley, J. R. Lindle, C. L. Canedy, I. Vurgaftman, and J. R. Meyer, Appl. Phys. Lett. **88**, 191105 (2006).
[10] L. Sirigu, R. Terazzi, I. Amanti, M. Giovannini, J. Faist, A. Dunbar, and R. Houdré, Opt. Express **16**, 5206 (2008).
[11] O. Painter, R. K. Lee, A. Scherer, A. Yariv, J. D. O'Brien, P. D. Dapkus, and I. Kim, Science **284**, 1819 (1999).
[12] H. G. Park, S. H. Kim, S. H. Kwon, Y. Ju, J. K. Yang, J. H. Baek, S. B. Kim, and Y. H. Lee, Science **305**, 1444 (2004).
[13] S. W. Chen, T. C. Lu, Y. J. Hou, T. C. Liu, H. C. Kuo, and S. C. Wang, Appl. Phys Lett. **96**, 071108 (2010).
[14] P. S. Weng, T. T. Wu, T. C. Lu, and S. C. Wang, Opt. Lett. **36**, 1908 (2011).